ISSN 0016-8521, Geotectonics, 2024, Vol. 58, No. 3, pp. 368–383. © Pleiades Publishing, Ltd., 2024.
ISSN 0016-8521, Geotectonics, 2024. © Pleiades Publishing, Ltd., 2024.

Geological Position, Structural Manifestations of the Elbistan Earthquake and Tectonic Comparison of Two Strongest 06.02.2023 Seismic Events in Eastern Turkiye

Ya. I. Trikhunkov[a, *], H. Çelik[b], V. S. Lomov[a], V. G. Trifonov[a], D. M. Bachmanov[a], Y. Karginoglu[b], and S. Yu. Sokolov[a]

[a] *Geological Institute, Russian Academy of Sciences, Moscow, 119017 Russia*

[b] *Firat University, Engineering Faculty, Department of Geological Engineering, Elazig, 231119 Turkiye*

**e-mail: jarsun@yandex.ru*

Received December 28, 2023; revised May 17, 2024; accepted June 26, 2024

Abstract—The Elbistan (Chardak) earthquake with magnitude $M_w = 7.5$ or 7.6 happened in Eastern Anatolia on 06.02.2023 at 10:24 UTC, following the strongest in the region of East Anatolian (Pazarcık) earthquake with $M_w = 7.8$ which occurred on the same day at 1:17 UTC to the south of the region. The Elbistan earthquake activated adjacent segments of the Chardak and Uluova faults with left-lateral strike-slip displacements. The resulting seismic ruptures have a total length of 190 km, of which 148 km are represented by sinistral lateral slip. Their maximum amplitude of 7.84 m was recorded 8 km east of the epicenter. The strike-slip seismic ruptures of the Elbistan and East Anatolian earthquakes represent exposure of their focal zones on the land surface. Both earthquakes exceed average values of these parameters for continental earthquakes of strike-slip type in terms of focal zone sizes and amplitudes of seismic displacements. At the same time, both sources do not propagate deeper than the upper part of the crust (16–20 km). Ophiolite assemblages covering the same depths are widely spread in the area of focal zones of both earthquakes. Two maxima were found in the distribution of seismic strike-slip displacement along the epicentral zone of the Elbistan earthquake (i) amplitudes of 5.7–7.84 m in the Chardak fault zone and (ii) amplitudes of 3.5–5.1 m in the Uluova fault zone. Both maxima coincide with the areas of ophiolites or their contacts with basement rocks. In crystalline basement rocks, the sinistral strike-slip amplitudes are significantly reduced. We attribute the increased values of focal zone sizes and displacement amplitudes of both earthquakes to the rheological features of ophiolites, which increase a possibility rocks slipping during seismic movements. We explain the fact that the sources of both earthquakes cover only the upper part of the crust by the uplift of the top of rocks with reduced *P*-wave velocities, including the upper mantle and the lower part of the crust, and interpret them as heated rocks with reduced strength.

Keywords: Elbistan earthquake, Eastern Anatolian earthquake, Chardak and Uluova active fault zones, seismogenic displacements, sinistral strike-slip fault, ophiolites, depth of focal zone, basement, Earth's crust

DOI: 10.1134/S0016852124700250

INTRODUCTION

A series of tragic and, at the same time, unique seismic events shook Eastern Anatolia on 06.02.2023. The Elbistan (Chardak) earthquake with a magnitude of 7.5 [29] (or $M_w = 7.6$ [11]) occurred at 10:24 UTC, 9 hours after the strongest East Anatolian (Pazardzhik, [30]) earthquake with a magnitude of $M = 7.8$ occurred 96 km to the south [3].

A similar combination of two earthquakes of such high magnitude in two adjacent fault zones, one of which was previously considered inactive, had not been recorded before in the Eastern Mediterranean and the Middle East.

According to the US Geological Survey and Turkish sources, the epicenter of the Elbistan earthquake is localized in the southern wall of the Chardak fault 20 km south of Elbistan [11, 29]. The depth of the hypocenter is estimated at 7.4, 5 or 13 km [10, 11, 29].

After the earthquake, a dense cloud of aftershocks appeared, elongated along the Chardak and Uluova faults at a distance of ~200 km. The close depths of the hypocenters are also determined in the strongest aftershocks.

During the Elbistan earthquake neighboring segments of the Chardak and Uluova fault zones were activated, and the Uluova fault had been previously considered inactive [7] (Fig. 1).

The seismic ruptures that occurred along a 148 km long section resulted in left-lateral strike-slip displacements.

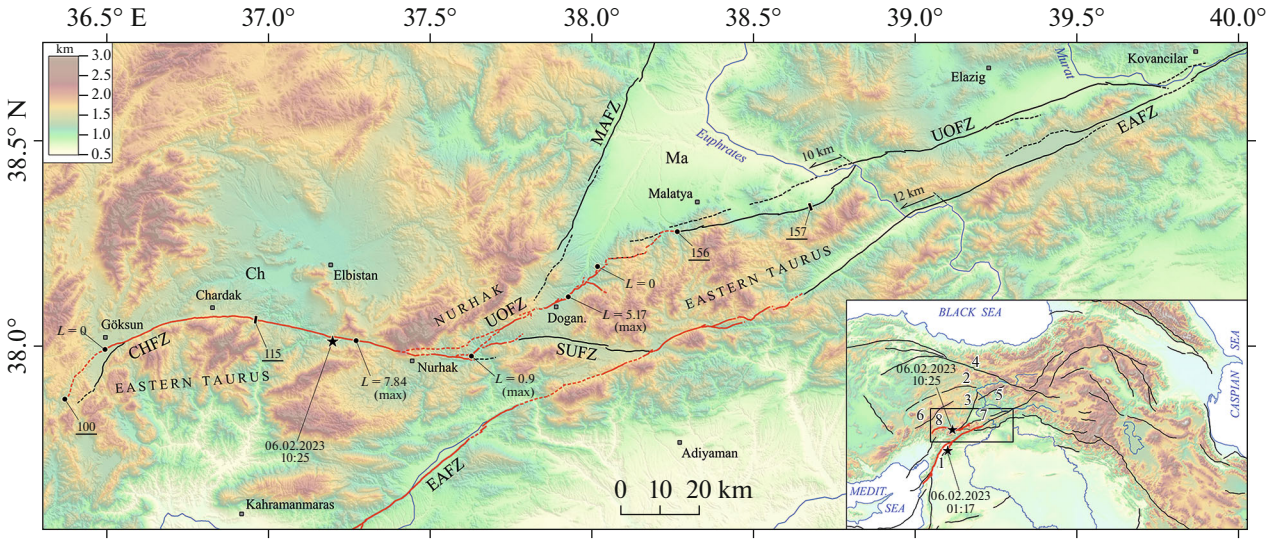

Fig. 1. Active fault zones of the Eastern Anatolia, Turkiye (after [15]). *Earthquakes*: occurred on 06.02.2023 (asterisks). *Fault segments*: activated (in red) and unaffected (in black) by earthquakes on 06.02.2023. *Faults*: CHFZ, Chardak; UOFZ, Uluova; EAFZ, East Anatolian zone; MAFZ, Malatya; SUFZ, Surgu. Epicenters of Elbistan and Pazarcık (East Anatolian, Kahramanmarash). *Depressions*: Ch, Chardak; Ma, Malatya. In the inset (faults): 1, East Anatolian zone; 2, Deliler; 3, Malatya; 4, North Anatolian zone; 5, Ovacık; 6, Sariz; 7, Uluova; 8, Chardak. Indicated: observation points with their numbers or maximum amplitudes (L) of left-shift displacements (m).

Despite the fact that the energy distribution of numerous aftershocks along the fault lines of Chardak and Uluova is proportional to the distribution of the magnitude of seismogenic displacements, movement along these faults occurred during and immediately after the main shock [3]. With such a small depth of the hypocenter, the seismic fractures that have arisen can be considered as exits of seismogenerating ruptures of the upper part of the earth's crust to the earth's surface and indicate the horizontal dimensions of the focal area.

The purpose of this article is to present and analyse the seismogenic ruptures that occurred during the Elbistan earthquake on 06.02.2023, to determine the tectonic position of this earthquake and its geodynamic settings.

GEOLOGICAL SETTING

The ophiolite assemblage rocks (peridotites of varying degrees of serpentinization, gabbroids, basalt lavas, fields of basalt dikes and ophiolitic mélange) play an important role in the structure of the upper part of the Earth's crust of Eastern Anatolia.

The defining elements of the Mesozoic–Cenozoic tectonic zonality are two zones of ophiolite sutures. In the north, these are the eastern segments of the Izmir–Ankara–Erzincan suture, which continues eastward with the ophiolites of the Bazum range and the Sevan-Akerin zone of Armenia. In the south—the suture of the Southern Taurus, which reaches the Iskenderun Bay in the west and continues with the structures of the southern frame of the Cyprus Arc, and in the east passes into the suture of the Main Thrust of Zagros [1, 13, 24, 28] (Fig. 2).

The formation of oceanic crust, represented by the ophiolites of the northern suture, began in the Late Triassic. Subduction continued from the Middle Jurassic and was replaced by a collision no later than the Turonian–Campanian [5, 8, 21, 23, 26].

The South Taurus suture marks the development of the Neotethys basin, where subduction began in the Cretaceous, and the closure of its relics and the beginning of the collision occurred in the Late Eocene–Oligocene [1]. Both main sutures are accompanied by ophiolites opened in tectonic windows in the rear of the overhung sutures and obducted ophiolite allochthones in their front.

The fragments of the 2nd-order ophiolite zones separating microplates and blocks have been preserved between the main sutures [22]. These include the branch of the northern suture, which separates from it on the western edge of the Erzurum depression, follows east to the city of Kagizman and further southeast along the southwestern shore of the lake Urmia, where it merges with the extension of the South Taurus Suture. This ophiolite zone separates the Tauride microplate from the fragmented western blocks of the Iranian microplate [28]. Seismically activated in 2023 the Chardak and Uluova faults are located inside the Tauride microplate north of the South Taurus Suture separating the microplate from the Arabian Plate.

The metamorphosed basement of the Taurids is dated to the Paleozoic–Early Triassic.

The basement of the Arabian Plate, exposed in its southwestern part, is of Precambrian age. In the

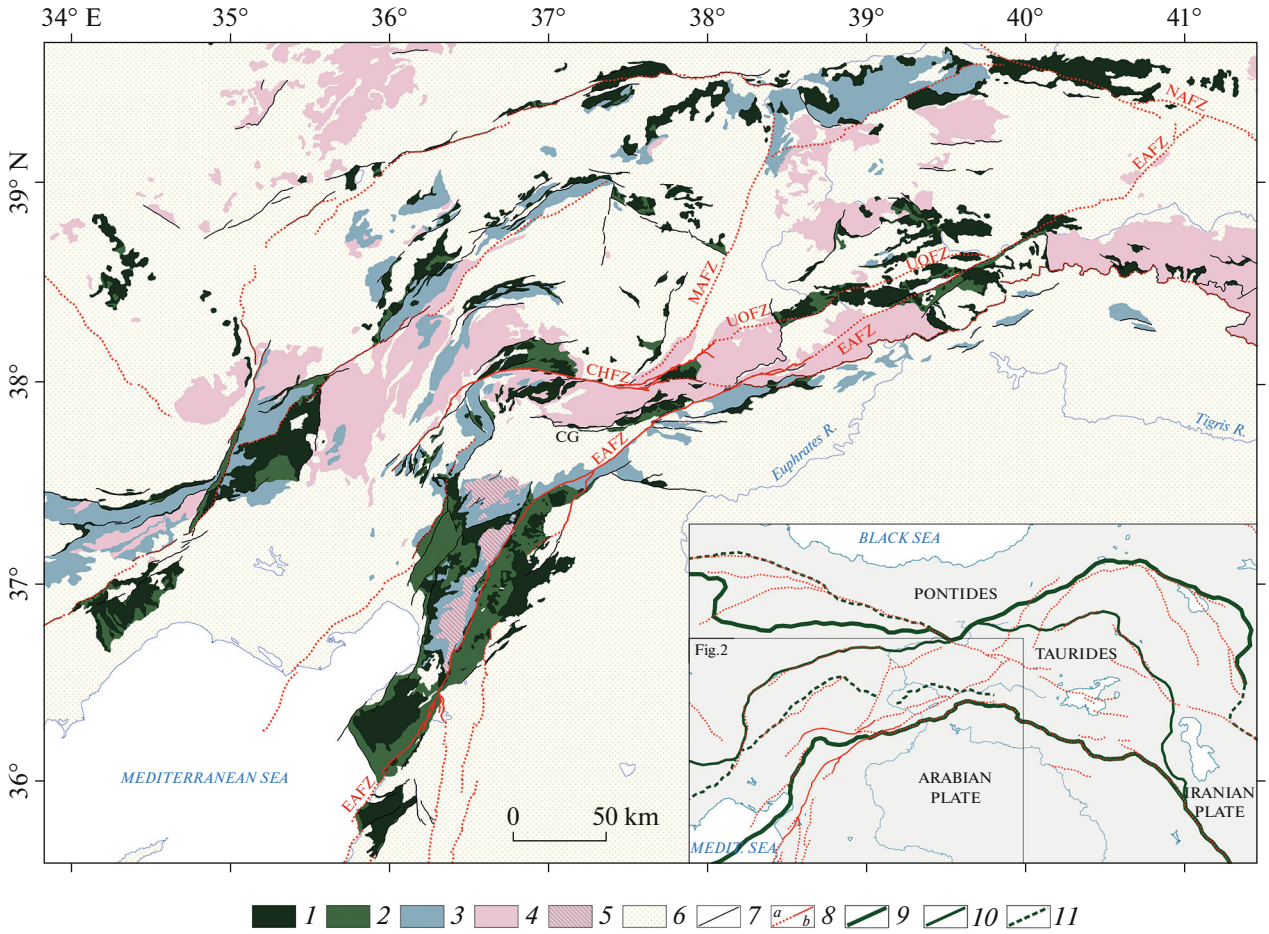

Fig. 2. Correlation of outcrops of crystalline basement, ophiolites and active faults of the inner segments of the Alpine-Himalayan belt in Eastern Anatolia and Transcaucasia, (after [9, 10, 15]). In inset: sutures of Eastern Turkey, Transcaucasia and Northwestern Iran separating plates and microplates (lines in green); CG, Chaglayancerit section with ophiolite suture of Neotethys. *1*, ophiolites exposed; *2*, ophiolites assumed to be under young sediments; *3*, complex of Middle Triassic–Cretaceous sediments; *4*, outcrops of metamorphic basement (in the Taurides, Malatya Formation); *5*, lower horizons of the platform cover of the Arabian plate (Cambrian–Ordovician); *6*, Maastrichtian and Cenozoic; *7*, faults; *8*, active faults (by earthquakes on 06.02.2023): *a*, unaffected; *b*, activated (fault segments); *9*, main sutures of Izmir–Ankara–Erzincan-Sevan and South Taurus; *10*, sutures separating microplates located between the main sutures; *11*, inferred sutures.

north–west of the plate, near the southwestern part of the focal zone of the Pazarcık (East Anatolian) earthquake, Cambro–Ordovician terrigenous and carbonate deposits of the platform type were uncovered, confirming the Precambrian age of the basement [9].

The foundation of the Taurids and the lower horizons of the cover of the Arabian Plate are overlain by a complex of rocks from the Middle Triassic to the Cretaceous. In the Taurids the complex is represented by neritic limestones, and on the Arabian plate—by pelagic deposits (Fig. 2).

This indicates the heterogeneity of the Earth's crust at the northern edge of the Arabian Plate, where continental fragments were combined with oceanic, marked by pelagic sediments. A similar heterogeneity was revealed earlier for the northeastern edge of the Arabian Plate, where it predetermined the features of its subduction and subsequent isostatic vertical movements [17].

The southern suture, that is, the contact of the Taurids and the Arabian plate, has been studied in detail in the South Taurus thrust zone north of the Chaglayancerit town [1]. A series of nappes, gently inclined to the north, has been uncovered here, which is represented by the following structures (from top to bottom):

— cover and basement of the Taurides;

— Bulgurkaya breccias, consisting of fragments of Tauride rocks and cemented by pelagic sediments;

— ophiolitic mélange.

Traces of the sedimentary rocks of the Arabian Plate moving under this sequence were found below the section.

In the Pliocene–Quaternary, a system of active faults formed, which complicated the tectonic zonality of the region [7, 12] (Fig. 1, inset).

The largest is the East Anatolian left-lateral zone. This zone extends from Iskenderun Bay to the north-

east and adjoins there the North Anatolian right-lateral zone, which extends to the west and reaches the Marmara Sea. In the modern structure, the East Anatolian left-lateral zone partly acts as the boundary of the Arabian and Anatolian plates. The North Anatolian zone bounds the Anatolian Plate from the north.

Within the tectonic wedge between the East Anatolian (left-lateral) and North Anatolian (right-lateral) fault zones in Eastern Anatolia, there are several large active faults of the second order. One of them is the sublatitudinal left-lateral Chardak fault. In the western part, this fault bends to the southwest and passes into a submeridional echelon sinistral faults of the southwestern strike, reaching the northwestern shore of Iskenderun Bay. At the eastern end, the Chardak fault branches off. To the east, it is continued by the Surgu fault, adjacent to the East Anatolian zone in the vicinity of Chelikhan town.

Koç et al. [18] united the Chardak and Surgu faults under the name "Surgu". In our opinion, these faults are not a single structure, and we give their names in accordance with the map of active faults of Turkiye [7].

The Uluova fault branches off to the northeast from the Chardak fault, which extends parallel to the East Anatolian zone and approaches it in the vicinity of Kovancılar town (Fig. 1).

The Uluova fault is considered as an older northern boundary of the Arabian Plate [4]. Before the Elbistan earthquake, the fault was considered inactive. It is not reflected on the map of active faults in Turkiye [7] and even in the work [2] on earthquakes in 2023. However, during the Elbistan earthquake on February 6, 2023, the latitudinal part of the Chardak fault and the southwestern part of the Uluova fault were activated.

From the Chardak fault to the north-northeast lies the Malatya zone of the oblique faults (sinistral + normal). In turn, the Ovacık fault, adjacent to the North Anatolian fault Zone, separates from its northern part to the northeast (Fig. 1, inset).

In the north, the Malatya zone closes with the Deliler fault zone. It forms a convex arc to the northwest. The latitudinal northeastern part of the arc is characterized by the thrusting of the northern wall, and its more western part, extending to the southwest and further south-southwest, is characterized by left-lateral displacements. Between the Malatya and Deliler fault zones the Sariz fault of the northeastern strike with predominantly left-lateral displacements has been identified [7].

MATERIALS AND METHODS

To characterize the geological structure of the Elbistan earthquake focal area the field materials obtained by the authors and the literature data were used [1–4, 6, 7, 10, 12, 14, 17, 18, 22–24].

We have defined the distribution and conditions of ophiolite massifs from geological maps [9] and field data. Data on the main shock and aftershocks of the Elbistan earthquake were obtained from the Kandilli Observatory of Bogazici University (Turkiye) [11] and the Earthquake Hazard Program of the US Geological Survey [29].

Remote data on the propagation of seismic fractures and their preliminary mapping were carried out on the basis of detailed satellite images taken in the first days after the main earthquake [14]. The most informative were the pictures of snow-covered areas, where the ruptures appeared most clearly.

During the field work the parameters of seismic fractures, seismogenic displacements and secondary seismic dislocations that occurred during the Elbistan earthquake were studied in detail at the key sites of the Chardak and Uluova faults.

GPS navigators were used to coordinate the observation points. Measurements of the seismogenic displacements parameters were carried out using a geodetic equipment—Suunto Tandem high-precision liquid compass-clinometer, Nikon Prostaff-5 laser rangefinder, telescopic leveling rails, geodetic measuring tapes. Unmanned aerial vehicle (quadcopter) DJI Mavic Air Pro-2 has been used to detect and map seismic faults, determine kinematics and displacement amplitudes, and identify secondary seismic dislocations.

To assess the state of the Earth's crust and upper mantle of the study region a tomographic model of variations in *P*-wave velocities (δVp) relative to the average values at specified depths in (%) MITP08 was used [20]. The model has a spatial resolution of ~100 km in the regions of the upper mantle with the densest wave path and ~150 km in the lower mantle. In this model, volumes with negative δVp acquire a vertically layered appearance and a clearer expression of the hot roots in the lower mantle.

In the upper mantle, MITP08 is characterized by good resolution and realistic interpretation under orogenic belts, subduction zones and areas with a developed seismic network, to which the Middle East region belongs [11]. The δVp values have different interpretations—thermal, substantial and related to stress sensitivity. In this paper we have used the thermal model as the most reasonable one [20].

Negative values of δVp are interpreted as "hot" volumes of the mantle, heated and partially melted. Positive values are interpreted as "cold" volumes, lesser values of which characterize the background state of the mantle [25], and larger values >0.75%, these are slabs with significant positive deviations δVp.

The boundaries of the hot mantle volumes were determined by specifying a 3D isosurface of δVp, which outlines these volumes in space. If the value of δVp is selected at a deep negative level (for example, ≤–1%), then the isosurface can highlight only the most heated domains and does not show a system of channels supplying the matter from the superplume branch.

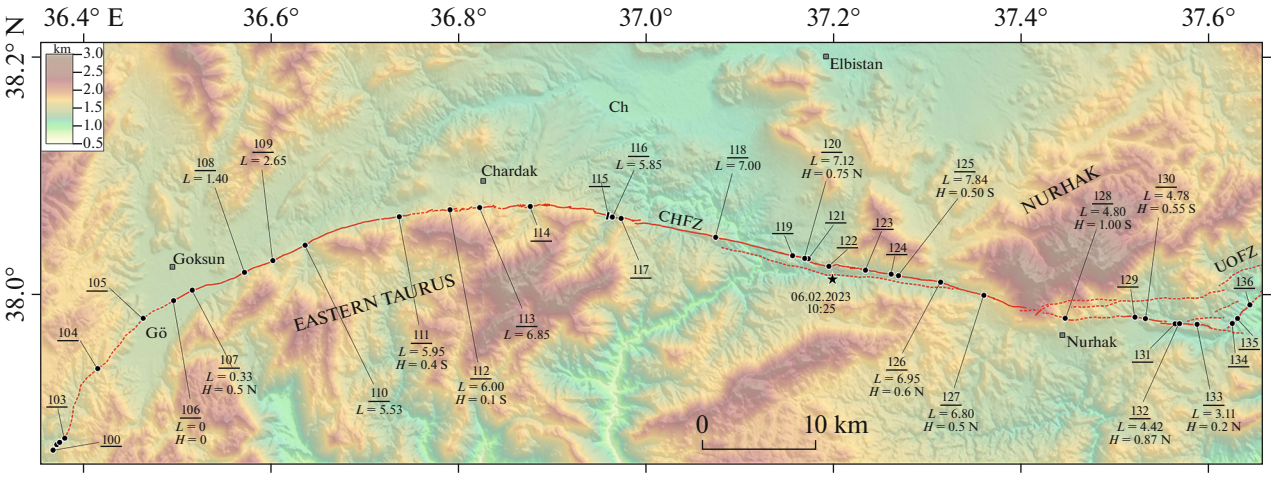

Fig. 3. Segment of the Chardak fault activated by the Elbistan earthquake (after [10, 15]). *Fault zones*: CHFZ, Chardak zone; UOFZ, Uluova zone. Depressions: Ch, Chardak; Gö, Göksun. Indicated: locally established seismic faults with left-lateral displacements (solid lines in red); seismic faults without lateral displacements and inferred faults (dashed lines in red); epicenter of the Elbistan earthquake (asterisk); observation points (circles in black) with their numbers and amplitudes of displacements (m); L, left shift; H, vertical shift (with indication of uplifted wall).

If the nominal value of the isosurface is selected at a small level near zero δVp, then link channels with the plume branch are visualized, but at the same time, there is a risk of adding random fluctuations to their shape at a noise level near zero average value δVp. Since the level of δVp in each heated area of the mantle is different, the nominal value of the isosurface for it is selected individually based on a stable display of its boundary with a significant variation in the nominal value of δVp.

For the research area such a range was obtained from –0.37 to –0.6%. The structural map of the heated mantle volumes top was constructed after calculating the 3D grid according to the MITP08 model [20] with their interpolation onto a grid of 10 km along the depth axis and 50 km along the horizontal axes. After that, the isosurface of the required nominal value was exported for the part outlining the heated volume from above. The surface shape of the lower part of the volume was not considered and was cut off after export.

RESULTS

Seismogenic Displacements during the Elbistan Earthquake

As a result of the Elbistan earthquake segments of the Chardak and Uluova faults between the Goksun (Kahramanmarash province) and Malatya (province of the same name) cities were activated. This fault zone runs along the northern foot of the Southeastern Taurus and its northern branch, the Nurhak Dagi ridge, in contact with the foothill depressions bordering the ridges from the north (Fig. 3).

According to the resulting seismic fractures, left-lateral displacements occurred over 148 km. Their maximum amplitude of 7.84 m was observed on the Chardak fault line 8 km east of the epicenter (Fig. 3, point 125). The total length of the seismic disturbance zone along the Chardak–Uluova fault line reaches 190 km, which almost coincides with the length of the aftershock cloud.

The western segment of the strike-slip displacement zone along the Chardak fault. The seismic fault zone begins 80 km west of the epicenter in the area of the village of Kuchukchamurlu. There are signs of activation of seismic fractures preserved from previous movements along the Chardak fault. The seismogravitational destruction of the Dibek ridge top in the extreme western foothills of the Eastern Taurus, composed of Middle Miocene limestones, is described (Fig. 3, points 100–103).

Dislocations are manifested by a series of micrograbens of the pull-apart type, formed along the axis of the ridge (Supplement 1: Fig. P1). The strike of the ruptures is 32°–35° coincide with the extension of the Chardak fault in this area.

Similar seismogravitational dislocations, as well as traces of co-seismic rockfalls, were noted by us in the western part of the Chardak fault on a 15 km stretch between observation points (hereinafter the point) 100 and 105 up to the entrance into the Goksun depression (Fig. 3).

Here the fault becomes elusive, since it is dispersed in the thickness of the alluvial filling of the depression. At point 107, we recorded the first (from the west) left-lateral displacement along the fault (Fig. 3).

The irrigation channel was shifted by 0.33 m in strike ∟60° when the northern wall was raised by 20–50 cm.

Further to the east–northeast, the amplitude of the sinistral displacements increases rapidly (Fig. 3, Suppl. l: Fig. P2, P3):

— 1.4 m at point 108 near the village of Karaakhmet;

— 2.65 m at point 109;

— 5.53 m at point 110 near the village of Kale-Salyan (13 km from the conditional western point of zero displacements along the Chardak fault).

On the sublatitudinal segment of the Chardak fault between points 111 and 117, the amplitude of the sinistral displacements is maintained in the range of 5–7 m (Fig. 3).

At point 111 (sinistral displacements by 5.95 m; strike is –45°), the fault dissects the massif of Late Cretaceous ophiolites and is characterized by the elevation of the southern Taurus wall of the fault by 0.4–2 m (Fig. 3).

The fault plane dips south towards the mountains at an angle of 60°, which suggests the presence of a reverse fault component of movements. A young stream has been formed along the renewed fault (Suppl. 1: Fig. P2, 111).

At the same time, due to the strike-slip deformation of a small hill at this observation point, the appearance of lifting the opposite wall is created.

At the point 114, the riverbed of the Esendere River, flowing down from the northern slope of the Eastern Taurus, is shifted to the left by 5.90 m (Fig. 3).

The fault extends along the foot of the ridge along the strike of 85°. The pebbly riverbed bar is dissected and displaced in the eastern side of the valley by the same amount. The old fault zone with a total width of several meters has been updated here. The vertical component of the displacements on the valley slope isn't obvious, however, the floodplain is deformed by 0.9 m with the elevation of the southern wall (Fig. 4).

The fault plane falls under the raised Taurus wall (dip direction is 175°, angle of dip—∟75°). Based on this, we can assume that the fault, in addition to the sinistral displacement, has a reverse-fault component. Note that everywhere, where the vertical component is fixed in the western segment of the strike-slip fault zone, the southern Taurus wall is raised.

At point 114, the modern rupture is formed at the contact of volcanogenic sedimentary rocks of the ophiolite association, composing the basement of the Goksun depression, and carbonate rocks composing the Eastern Taurus. Rocks in the contact zone have been subjected to cataclastic metamorphism and hydrothermal mineralization for a long time. In the calcite filling slickenside with horizontal striation are clearly expressed on the opened fault plane (Fig. 4).

The reverse-fault component of the displacements during the last movement is weakly manifested in the slickensides.

Expressive examples of movements during the Elbistan earthquake are presented at points 115–117 in the Karatut village (Fig. 4).

Here, similar to point 114, the fault zone is expressed in the cataclastically deformed mineralized rock—Lower-Middle Eocene volcanites, with a total width of 40–50 m. It accommodates both a modern rupture with a left-lateral displacement of 5.85 m (point 116) and 5.15 m (point 117), as well as traces of previous movements. They were opened in a roadcut in the form of fault pockets, where buried paleosols containing organic material (charcoal) selected for C14 dating, lie under a layer of modern soil (Fig. 5).

The epicentral segment of the strike-slip displacement zone. The epicenter of the Elbistan earthquake is located 20 km south of Elbistan town near the Chiftlikkale village at the intersection of the CHFZ and the valley of the Ceyhan River. Within the epicentral segment, at points 118–127, we recorded maximum left-lateral displacements exceeding 7 m (Fig. 3).

Left–lateral displacements occurred in Mesozoic ophiolites, which underwent secondary cataclastic and hydrothermal changes at points:

— 118—sinistral offset by 7 m; strike is –90°;

— 119—sinistral offset by 6.62 m; strike is –114°; the southern wall is raised by 0.6 m;

— 120—sinistral offset by 7.12 m; strike is –90°; the north wall is raised by 0.75 m.

At point 120 in the Chiftlikkale village, the sinistral offset by 7.12 m was measured by the deformation of the ravine talweg (Suppl. 1: Fig. P. 3).

Here, the fault dissects the ophiolitic melange massif with high level of secondary carbonate mineralization. This is the first of the points described by us, where the fault plane dips to the north at angles of 55°–80°, and is uplifted (thrusted) its north wall. At the same time, as at point 114, slickensides with a distinct left-lateral striation without vertical component are described here. A similar phenomenon of the absence of vertical striation with obvious vertical deformations of the surface was described by us earlier in the East Anatolian fault zone [3].

Seismic dislocations, atypical for the Chardak fault, occurred directly in the epicenter east of the Chiftlikkale village. If to the west and east of the epicenter the fault is manifested as the single straightened line of seismic ruptures, then at point 122 a right-echelon series of short ruptures of normal fault kinematics has formed, complicating the graben-like structure. We believe that such a structure in the epicenter arose as a result of left-lateral movement along the fault in combination with the impact of seismic waves, which were as powerful as possible and reached the surface at this point (Fig. 3).

Further east, within the epicentral segment of the Chardak fault, the sinistral displacements are maintained in the range of 6–7 m, reaching a maximum in

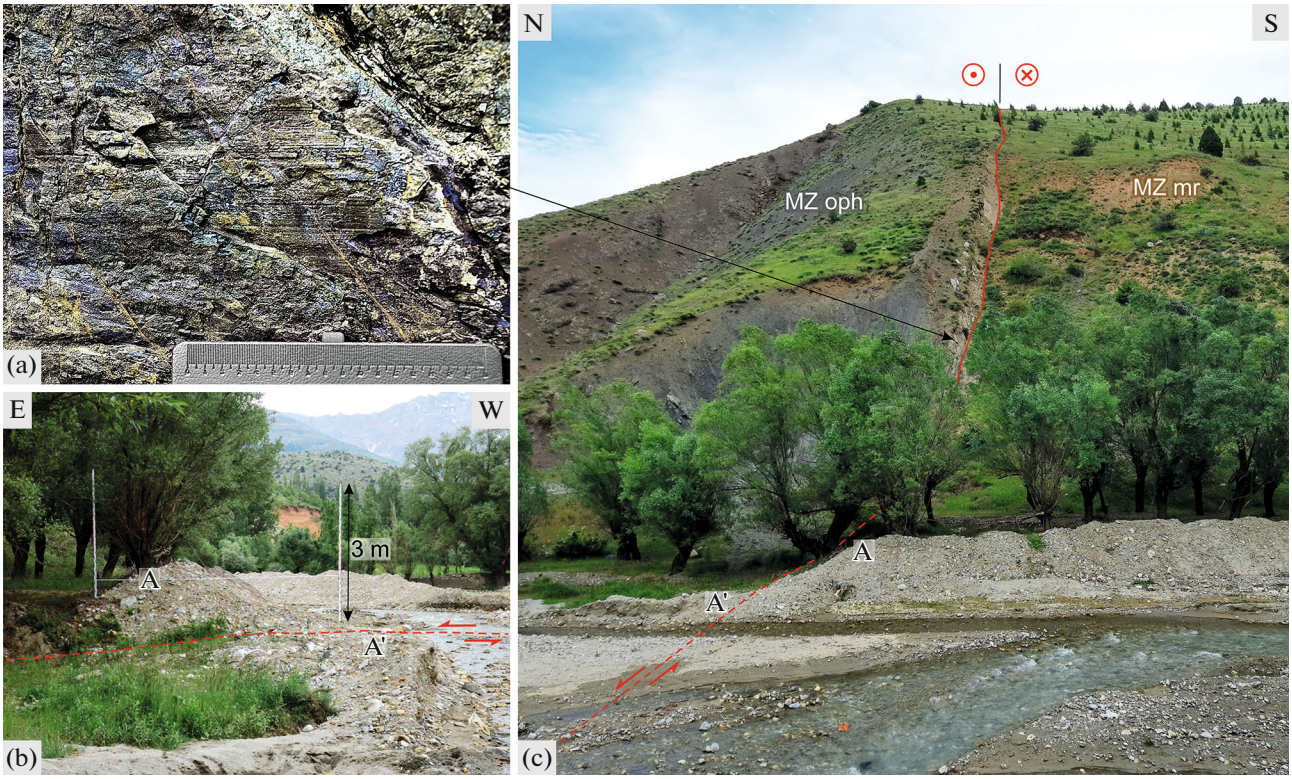

Fig. 4. Seismogenic disturbances in the Esendere River valley. (a) Slip mirror with left-lateral displacement hatching on the surface of the northern wall of the Chardak fault in the thickness of cataclastic altered mudstones of the volcanogenic-sedimentary ophiolite association; (b) left-lateral displacement of the riverbed gravel bar by 5.90 m at the fault strike azimuth of 85°, measured along the foot of the bar; (c) left-lateral strike-slip displacement of the valley side and the river bed along the Chardak fault with the southern wall uplifted by 0.9 m.

Fig. 5. Chardak fault zone in the Karatut Village. (a) Modern seismic rupture (line in red); (b) traces of different-age earlier displacements (line in black).

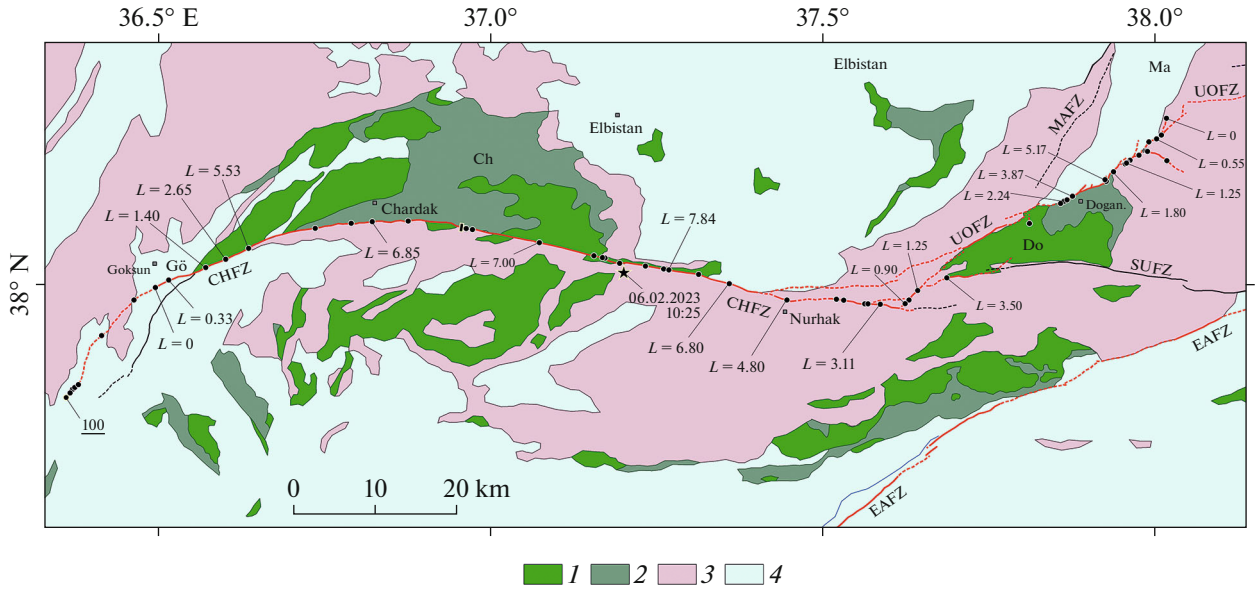

Fig. 6. Material complexes of Elbistan earthquake area. *1*, Ophiolites on the day surface; *2*, ophiolites assumed to be under the cover of young sediments; *3*, metamorphic rocks of the basement (Malatya Metamorphics); *4*, Mesozoic and Cenozoic sedimentary and volcanic deposits.

the Degirmenkaya village at point 125. The left-lateral deformation of the concrete base of the garden fence reached 7.84 m.

Further east for 15 km, the displacement values are maintained: at the point 126—a sinistral offset of 6.95 m, strike is 100°, the north wall is uplifted by 0.6 m; at the point 127—a sinistral offset of 6.80 m, strike is 100°, the north wall is uplifted by 0.5 m.

Further east, the displacement amplitudes drop sharply to values of 2–4 m. At the same time, at the point 127, we described the extreme eastern outcrop of Late Cretaceous ophiolites in the zone of the Chardak fault (Figs. 3, 6).

The eastern segment of the zone of sinistral displacements along the Chardak fault. East of point 127, the pattern of seismogenic displacements along the Chardak fault changes dramatically. The amplitude of the lateral displacement in this short ~18 km segment of the strike-slip zone is sharply reduced. If the amplitude was in the range of 6–8 m in the epicentral segment for ~30 km, then between points 128 and 133 it decreases from 4.8 to 3.11 m (Fig. 7).

The vertical component of the displacements here ranges from 0.2 to 1 m, the northern wall, in which the Nurhak-Dagi ridge is located, is uplifted.

North of the main fault zone digital relief models [15] show an expressive lineament along which movements could occur that took over part of the sinistral displacement amplitude (Fig. 6).

However, on the ground, the threefold intersection of the zone of this lineament in different parts of it did not reveal seismogenic disturbances. Additional ruptures were not reflected in the database [14], despite the fact that ruptures along the main fault line are clearly represented there.

The zone of sinistral displacements along the Uluova fault. The area between points 133 and 137 is an area of complex junction of the Chardak, Surgu, and Uluova faults (Fig. 6).

The amplitudes of sinistral displacements here decrease to a minimum. At point 134, a displacement of 0.9 m with strike 45° was measured when the northwest wall was uplifted by 0.3 m. At point 134 and beyond, all measured strikes of the ruptures change to the northeast, characteristic of the Uluova fault. The further spread of seismic fractures precisely to the northeast up to the vicinity of Malatya, and not to the east along the Surgu fault zone, is confirmed by our study. When moving in this direction from point 134, the displacement amplitudes begin to increase sequentially again, increasing to 2.2 m at point 136.

Along the entire length of the eastern segment of the Chardak fault from point 128 to point 136 on the Uluova fault, a sequence of Paleozoic–Mesozoic marbled limestones of the Malatya Metamorphics is widespread (Figs. 6, 7).

The situation changes at point 137, where a shift of 3.5 m with strike 42° was recorded when the northwestern wall of the Uluova fault was uplifted by 0.87 m. Here, seismic fractures disrupt the thickness of Mesozoic ophiolites again forming the Doganshehir depression (Figs. 6, 7).

The fault runs along the boundary of the depression and separates the ophiolites from the rocks of the Malatya complex composing the Eastern Taurus. The

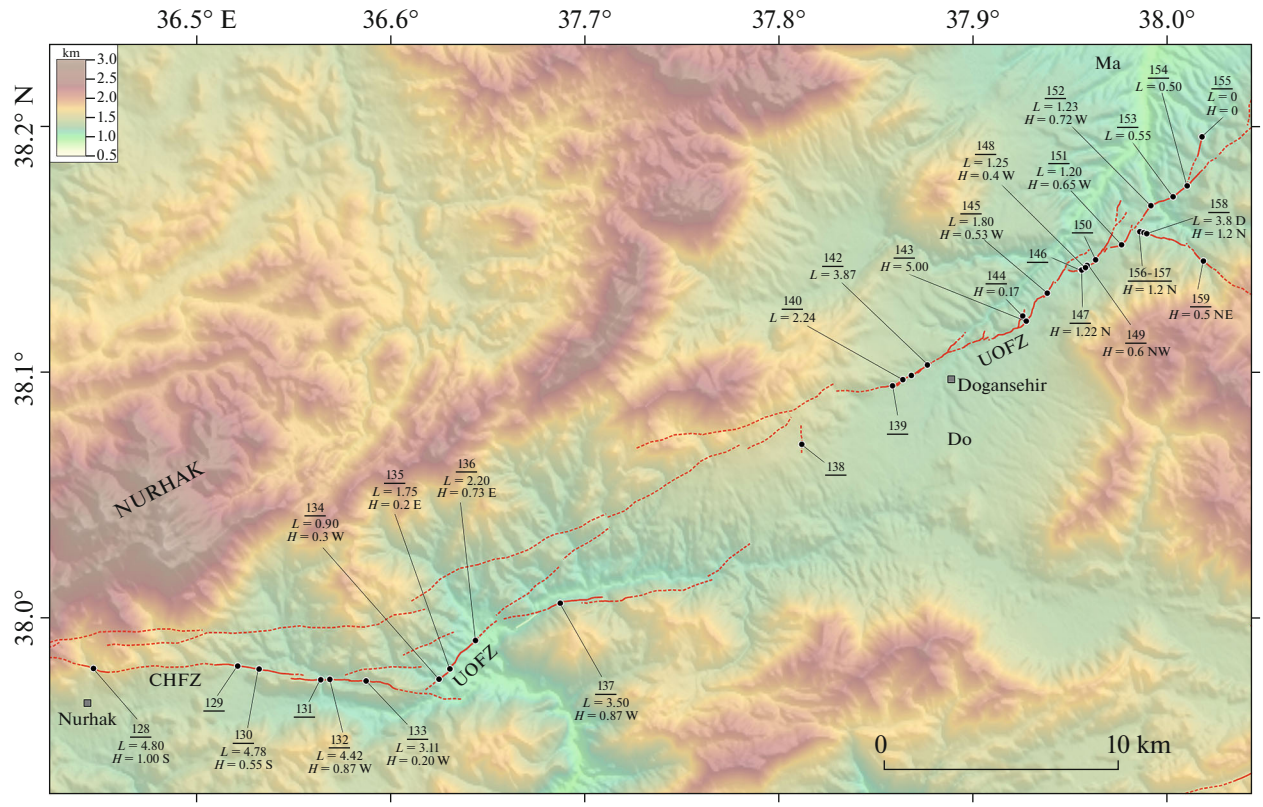

Fig. 7. Displacement zone along the Uluova fault (after [10, 15]). *Fault zones*: CHFZ, Chardak zone; UOFZ, Uluova zone. Depressions: Do, Doganshehir; Ma; Malatya. For notation—see Fig. 3.

left shift extends from this point to the east along the border of the ridge and the depression, but after a few kilometers it is completely lost. We are inclined to believe that the displacements here have affected the extreme western part of the Surgu fault, connecting the Chardak fault with the East Anatolian zone, and passing through point 137 according to data [9, 21] (Fig. 7).

In addition, on digital elevation models from the junction of the fault at point 137 through Surgu town passes an expressive lineament corresponding to the fault of the same name [15].

Our numerous searches for the continuation of seismogenic ruptures along the Surgu fault east of point 137 during the field studies and when analyzing satellite images of the snow-covered surface taken in the first days after the earthquake did not yield results [14]. It was also not possible to detect seismogenic ruptures north of point 137 in the western part of the Doganshehir depression (Figs. 6, 7).

Probably, for the same reason, there is no mention of strike-slip displacements along the Uluova fault [2].

However, to the northeast in the central part of the Doganshehir depression at point 138, we detected left-lateral displacements of 0.9 m. The seismogenic gap here extends to the north, and there are signs of normal fault in it—the fault plane is tilted to the west, towards the lowered wall (Fig. 7).

To the northeast, starting from point 139, on the northern side of the depression in the vicinity of Doganshehir, there is a continuous band of ruptures with stable sinistral displacements (Fig. 7).

The ruptures follow the contact of the ophiolites composing the depression with the marbles of the Malatya Metamorphics, composing the southern foothills of the Nurhak Dagi ridge. Between points 139 and 142, the displacements increase sequentially from 1.4 to 3.87 m. The maximum displacement along the Uluova fault is described at points 143 and 144 on two adjacent branches of the fault (Fig. 7).

Near the Chiglik village the landslide block was displaced by 5 m (Fig. 8, 143).

The left-lateral movement along the adjacent parallel branch of the fault at point 144 was 0.17 m. Thus, the total displacement along the Uluova fault (strike is 30°) at points 143 and 144 reached 5.17 m (Fig. 7).

Further to the northeast, in the segment between points 145 and 155, seismic fractures extend beyond the Doganshehir depression and dissect the northern slope of the Eastern Taurus, composed of marbles and crystalline shales of the Malatya Metamorphics (Fig. 6).

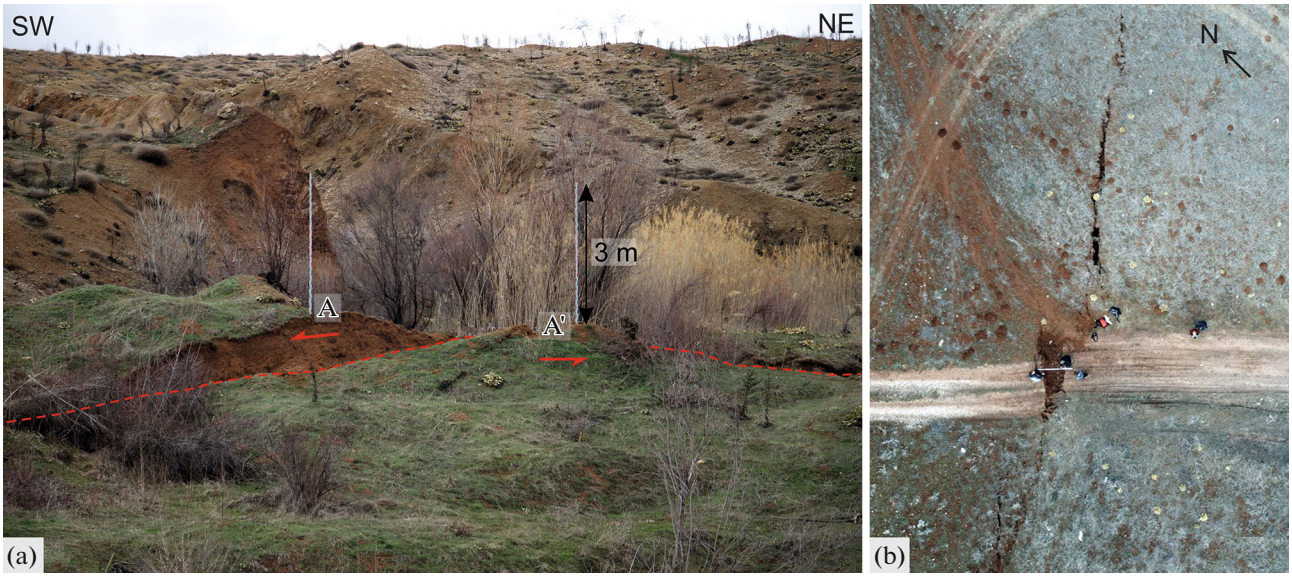

Fig. 8. Sinistral displacements along the Uluova fault. (a) Displacement of the landslide body by 5 m along the Uluova fault near Chiglik village; (b) displacement of the roadbed and the zone of seismogenic dislocations along the Uluova fault.

Here the fault begins to branch; seismic fractures form a tree-like structure in plan (Figs. 6, 7).

Strike-slip displacements are noted along the main line of the fault zone, but their amplitude between points 144 and 145 decreases sharply. At point 145 it is 1.8 m, at points 148–152 it is maintained at 1.2 m, at points 153 and 154 –~0.5 m (Fig. 7).

The weakly marked fracture reaches point 155, the strike-slip displacements along which are not marked.

Short lateral ruptures extending north from the fault show signs of normal faults. Numerous small depressions of the pull-apart type, similar to depressions at points 100–103, are marked between them and the main fault zone (Suppl. 1: Figs. S1–S3).

Between points 151 and 152 to the southeast, almost at an angle of 90 degrees to the main fault line, an amplitude Eskikoy reverse fault branches off (Fig. 6).

We have not detected strike-slip displacements along this fault. At points 157 and 159, there are expressive upslope slickensides with vertical striation on the fault plane dip to the northeast at an angle of ~60°. The maximum amplitude of the northeastern fault wall uplift is 1.2 m described at points 156–158 (Fig. 7).

The Chardak and Uluova Faults in the Quaternary Period

The Quaternary history of the development of fault zones activated during the Elbistan earthquake of 06.02.2023 has been poorly studied and the available data are contradictory. Most researchers consider the Chardak and Uluova faults as branches of the East Anatolian zone, characterized by left-lateral displacements [2, 4, 6, 7].

However, it is argued that before the Elbistan earthquake, this zone had dextral kinematics [18]. Our remote and field studies of both fault zones revealed a series of left-lateral displacements of the drainage system.

Morphotectonic signs of Quaternary sinistral displacements along the Chardak fault were found by us in its western and epicentral segments. The valleys of the three small right tributaries of the Goksun River, located between the town of the same name and the Chardak village, experienced left-lateral displacements during the Quaternary. The amplitude of the left shift between points 111 and 113 increases sequentially 300 → 500 → 800 m (Figs. 3, 9a).

A characteristic feature of the development of valleys transverse to the strike-slip zone is the adjunction of short left the 1st-order tributaries at the points of the valley exit from the shifted section. In the three displacement sites under consideration, the valleys of these tributaries assume the role of main valleys at the present stage of development (Fig. 9a).

Displacements with an amplitude of 1000–1200 m were detected in the valleys of the short left tributaries of the Ceyhan River between points 115 and 118 (Figs. 3, 9b).

In the range from 100 to 500 m, we estimate numerous left-lateral displacements of the short right tributaries of the Nargile River (a tributary of the Ceyhan River) at the southern foot of the Nurhak-Dagi ridge between the Chiftlikkale and the Barish villages in the epicentral segment of the fault zone (Fig. 9c).

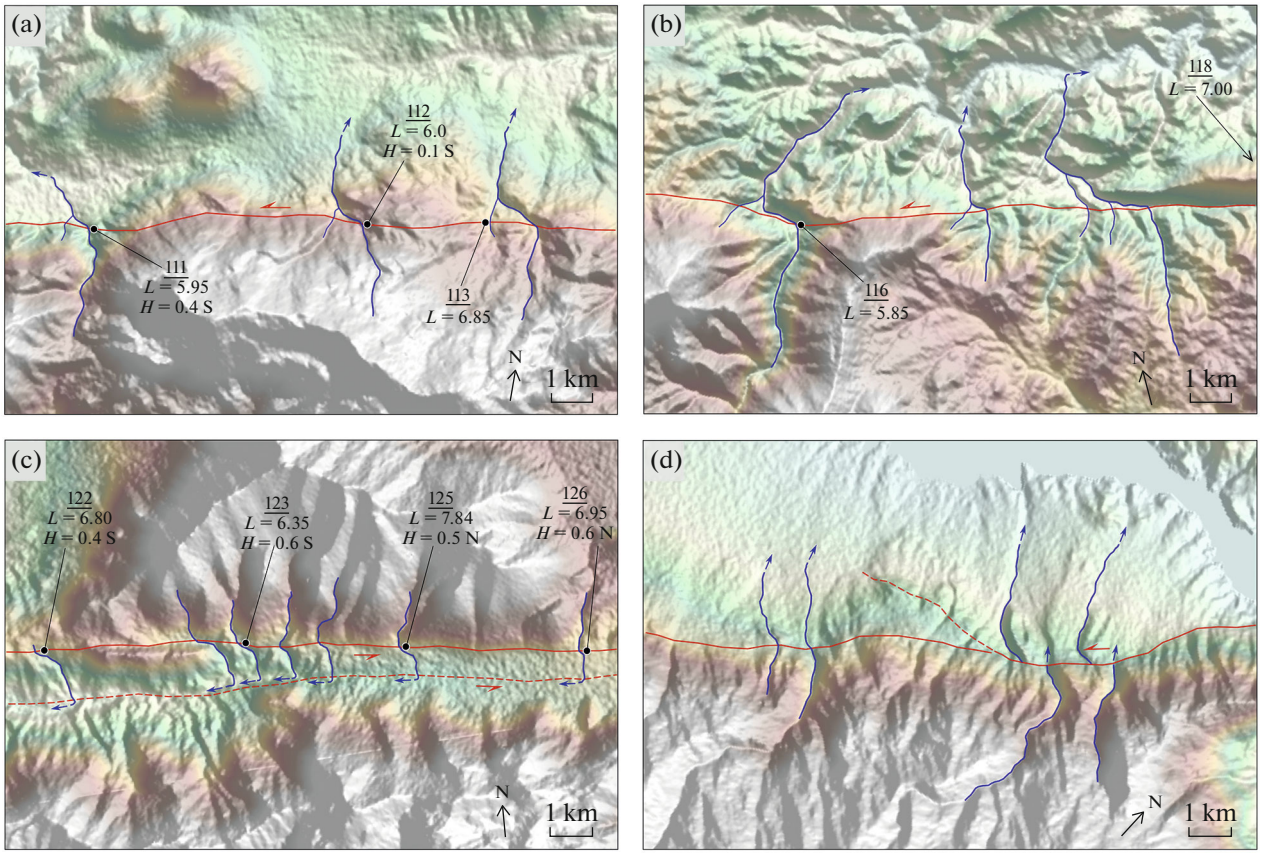

Fig. 9. Manifestations in relief of Quaternary left-lateral shifts along the Chardak and Uluova faults (after [10, 15]). *Faults*: (a)–(c) Chardak; (d) Uluova.

We explain such different amplitudes of displacements in neighboring sections of one fault zone by splitting it into two (or more) parallel branches active at different stages of the zone development. During the Elbistan earthquake movements occurred along the northern branch of the zone forming the foot of the Nurhak-Dagi southern slope. Judging by the deformations of the drainage system, previous movements also took place there. However, their relatively small amplitudes and the presence south of the latitudinal straightened valley of the Nargile River, stretched parallel to the band of modern ruptures, make us suggest that previous displacements occurred along this more southern branch of the fault (Figs. 3, 9c).

Morphotectonic signs of quaternary left-lateral displacements along the Uluova fault were revealed by us to the northeast of its western segment, activated during the Elbistan earthquake. The deformations of the Euphrates River tributaries in the east of the Malatya province are clearly expressed. We have presented sinistral displacements of two neighboring valleys of the right tributaries of the Euphrates River with an amplitude of ~0.8 km (Figs. 8, 9d).

These displacements are caused by movements along the young southern branch of the Uluova fault, extending northeast from point 156 and confirmed by trenching at point 157 (Fig. 1).

The left-lateral displacements of two parallel valleys 9 km southwest show significantly smaller amplitudes. We explain this discrepancy by the realization of movements along the branch of the fault of the northwestern strike (Fig. 9d).

The highest amplitude displacements are associated with long-term sinistral deformations of the Euphrates River valley at the place of its exit from the Malatya depression and entry into the Eastern Taurus area. In this section the valley is crossed by a rectilinear lineament of the Uluova fault zone main branch (Fig. 1).

Although the valley is occupied by the Karakaya reservoir within the Malatya depression, its talweg displacement can be estimated at 10 km.

In 20 km to the southeast, we detected a left-lateral displacement of the Euphrates River valley along the East Anatolian zone with an amplitude of 12 km for the last 1.2 my [27]. Thus, the total displacement of the Anatolian plate relative to the Arabian plate along both fault zones is estimated by us at 22 km during the existence of the antecedent valley of the Euphrates River in this section.

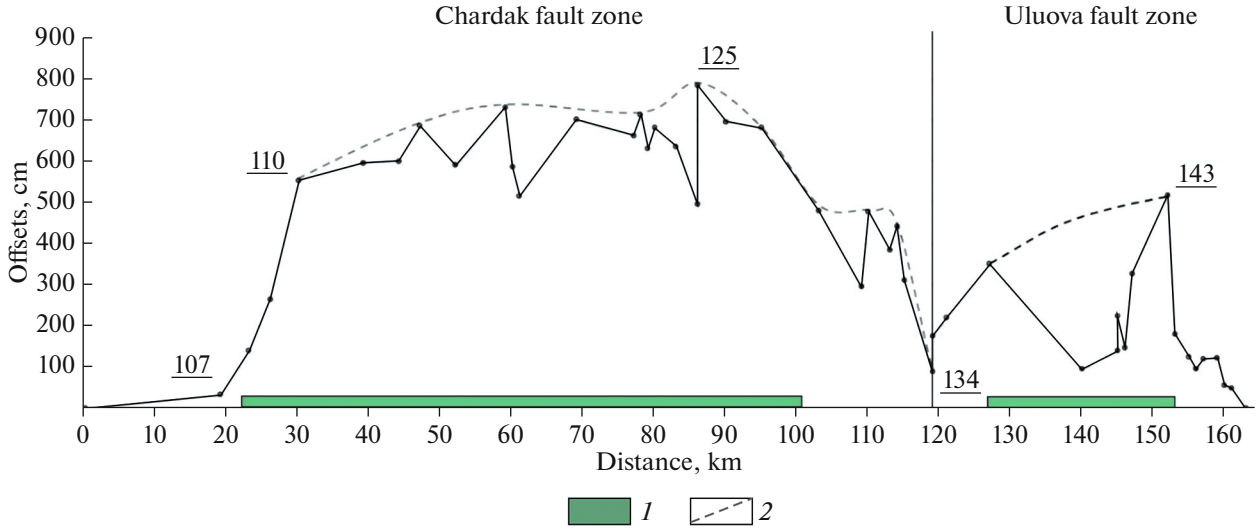

Fig. 10. Graph of distribution of left-lateral displacements along the Chardak and Uluova faults. *1*, Ophiolite outcrops; *2*, approximating curve.

DISCUSSION

Recent Kinematics of the Chardak and Uluova Faults and Analysis of the Distribution of Seismogenic Displacements

In the west of the Chardak fault during the Elbistan earthquake on February 6, 2023, for 20 km between points 100 and 107, only the renewal of old seismic fractures occurred (Fig. 3).

Here only vertical displacements of mainly normal fault kinematics are expressed without signs of strike-slip displacements (Suppl. 1: Fig. P1).

The minimum value of 0.33 m of the sinistral offset that occurred after the Elbistan earthquake was fixed at point 107. To the east, the strike-slip amplitude increases non-linearly and reaches 5.53 m after 10 km at point 110 (Fig. 10).

After reaching this value, the displacement graph reaches a plateau with average values of ~6.5 m. In this case, the graph line is a sawtooth curve. We explain the areas of reduced values of offsets between neighboring peaks by incomplete field data. Perhaps this is due to the implementation of left-shift displacements along the auxiliary faults not found in the field. In view of this, an approximating curve was introduced into the graph, emphasizing the plateau with offset values of ~6–7 m.

In all the considered points of the graph within the plateau, starting from point 108, the Chardak fault is embedded either in the thickness of Mesozoic ophiolites or in their contact with metamorphic rocks of the Eastern Taurus (Figs. 6, 10).

The fault forms the boundary of the Taurus Ridge and a flat depression composed of ophiolites, stretching along its northern foot from the town of Goksun to the town of Ekinozu. Further east, within the epicentral segment of the Chardak fault, the sinistral displacements remain in the range of 6–7 m, reaching a maximum of 7.84 m 8 km east of the epicenter at point 125 in the Degirmenkaya village. To the east, at points 126 and 127, the displacement values are in the range of 6.95–6.80 m, and further, between points 127 and 128, they drop sharply. At the same time, at point 127, we identified the extreme eastern outcrop of ophiolites in the Chardak fault zone (Figs. 6, 10).

At the eastern end of the fault between points 128 and 133, the average left lateral offset value is 3.9 m. An intermediate minimum of 0.9 m of strike-slip displacements was detected at point 134 in the west of the Uluova fault. We explain such a sharp drop in the offset amplitude by a complex branching in the junction zone of the Chardak, Uluova and Surgu faults. Further to the northeast along the mainline of the Uluova fault, the displacements begin to increase again.

The Surgu and Uluova faults, framing the Doganshehir depression from the south and north, similar to the Chardak fault, are formed down by the contact of ophiolites composing the basement of the depression and metamorphic rocks of the Malatya Metamorphics composing the surrounding ridges (Fig. 6).

The displacements first affected the Surgu fault at point 137, but then abruptly moved to the northern side of the depression—to the Uluova fault, also formed at the contact of ophiolites and metamorphic rocks composing the Nurhak Dagi ridge. Here, near the Chiglik village, at point 143, the displacements reach the second peak of 5.17 m, and then, at the exit from the Doganshehir depression, they sharply decrease to average values of ~1 m and disappear at point 155. At the same time, conditions of local extension probably arose inside the depression composed of ophiolites and a right-echelon

series of short meridional normal faults was formed—one of them was recorded by us at point 138 (Fig. 7).

Thus, there was a sharp increase in the amplitudes of left-lateral displacements at the contact or in the thickness of ophiolites, composing mainly depressions, and an equally sharp decrease in displacements in areas composed of a complex of metamorphic rocks forming ridges. At the same time, fault zones in the ophiolite thickness, as well as at their contacts, are expressed in straight lines and on the ground have a width of several meters to the first tens of meters (Fig. 6).

Within the areas composed of metamorphic rocks such as marbled limestones, marbles, crystalline shales, etc., faults are branching out against the background of a decrease in the amplitudes of strike-slip displacements (Fig. 6).

The tree-like pattern of ruptures of the Uluova fault zone between points 145 and 155 corresponds to the kinematic condition of compensation of sinistral displacements in the terminal part of the seismogenic displacement zone. In the southeastern wall of the sinistral fault zone, the compensating ruptures were reverse faults reflecting the compression conditions. The normal faults and gaps dominating the northwest wall reflect the extension.

The vertical component of the displacements along the main fault lines of the Chardak and Uluova faults varies. We believe that local variations of the dip angle and direction of the faults are determined by morphotectonics. For example, in the contact zone of the Eastern Taurus and the Goksun depression, the southern Taurus wall is raised at points 107–119, under which the fault plane dips steeply. In the epicentral region at points 120–127, where the Nurhak Dagi ridge is located in the northern wall of the fault, the fault plane dips steeply under it. Such variations of the dip angle and direction of the described seismogenic faults confirm the subvertical dip of their planes, which deviates only slightly from ∟90°. This is also evidenced by the fact that for many tens of kilometers the Chardak fault, accurately recorded by us from satellite images of the snow-covered territory in the first days after the earthquake [14], does not deviate upstream or downstream of the rivers crossing it, as is the case with gently dipping thrusts or normal faults.

Taking into account the vertical or subvertical dip of the seismogenic fault planes in the conditions of a regional compression and transpression, we consider them as vertical or subvertical strike-slip faults. These faults were formed at the late stages of the regional collision and cut through the previously existing structures of the gentle detachment.

The Role of Ophiolites in the Forming of the Elbistan and East Anatolian Earthquake Focuses

It was shown above that in ophiolites and at their contacts, the amplitudes of strike-slip displacements on February 6, 2023 increased sharply. Ophiolites are widespread in the focal areas of the Pazarcık and Elbistan earthquakes and in their vicinity (Fig. 2).

Some of the ophiolites belong to the South Taurus Suture, which in the section of the Chaglayancerit forms a tectonic slab, gently dipping to the north [1].

The contacts of many ophiolite massifs outcropping north of the suture show signs that the rocks of the crystalline basement or the Middle Triassic–Cretaceous complex are thrusting towards them. That is, the ophiolite autochthon is outcropping up in tectonic windows. These are, in particular, ophiolites exposed within the activated segments of fault zones: in the northern wall of the Chardak fault and the southeastern—of the Uluova fault [9]. The type of these ophiolites contacts indicates that they underlie the Taurides basement, and the amplitude of the detachment reaches tens of kilometers. At the same time, the thickness of the allochthonous Taurides basement can reach up to several kilometers.

The rocks of the ophiolite complex lying south-east of the South Taurus suture were obducted on the deposits of the Arabian Plate cover. These are serpentinites outcropped east of Antakya, ultrabasites of the Bassit, and ophiolites of Kurddag. The amplitudes of the thrusting of these allochthonous also reach tens of kilometers. Along with the mentioned ophiolites, fragments of ophiolite complexes may be present in the focal areas, obducted from the northern margin of the Taurides and/or the Izmir–Ankara–Erzincan suture (Fig. 2, inset).

The described ophiolite complexes, extrapolated to a depth in accordance with their exposition on the earth's surface, compose the upper part of the earth crust of the region, i.e. the same layers in which the hypocenters of the East Anatolian and Elbistan earthquakes and their strongest aftershocks with magnitudes of at least $M \leq 5$ are located.

We have shown that both earthquakes exceed the average values of the corresponding characteristics of strike-slip earthquakes of the same magnitude ($M \leq 7.5$) in terms of the total length of seismic fractures, maximum and average amplitudes of strike-slip displacements [3, 30].

We believe that such a large extent of focal zones and large values of seismogenic strike-slip displacements of both earthquakes are due to rheological features of ophiolites, which reduce friction and facilitate the sliding of rocks during seismic movements. It may also have been influenced by additional pressure caused by an increase in the volume of ophiolites during the transition of peridotite to serpentinite [16].

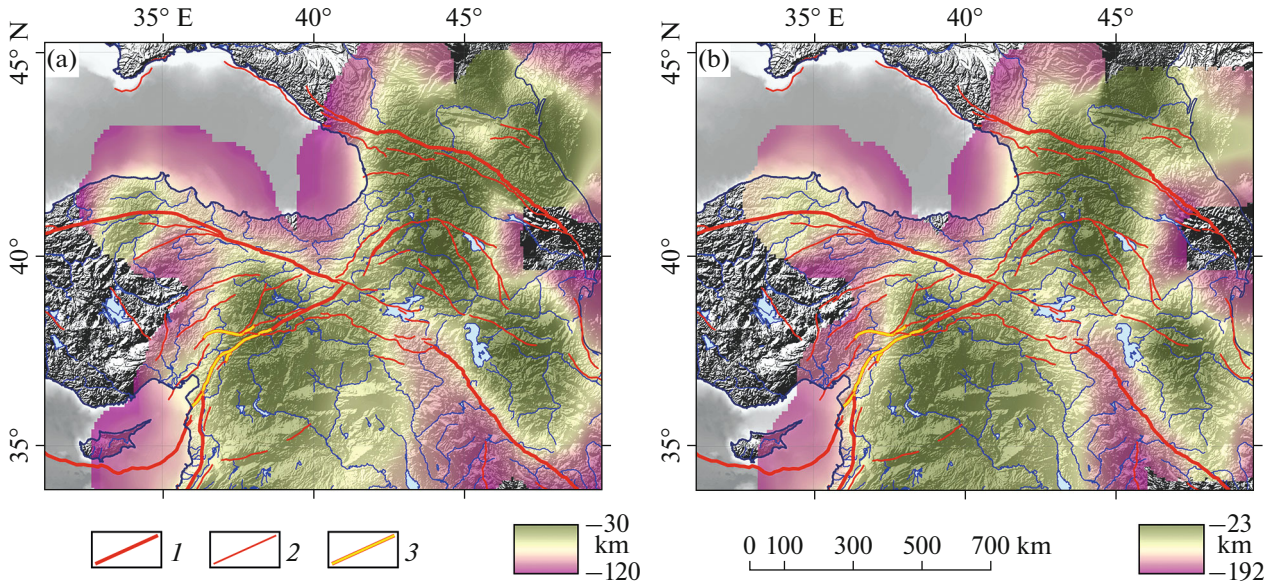

Fig. 11. Top position (km below sea level) of the lower crust and upper mantle volumes with reduced *P*-wave velocities beneath the Caucasus, Transcaucasia, Eastern Turkiye, Syria, Northern Iraq, and Northwestern Iran, calculated from the UU-P07 seismic tomography model (after [20]). The depths of the top of the lower crust and upper mantle with reduced *P*-wave velocities (color scale): (a) at $\delta Vp = -0.37\%$, (b) at $\delta Vp = -0.60\%$. *1–3* Active faults: *1*, largest; *2*, major; *3*, activated on 06.02.2023.

The State of the Earth's Crust and Upper Mantle in the Area of the East Anatolian Earthquakes on February 6, 2023

With the large size of the Elbistan earthquake focal area, the depth of the hypocenter was determined in the range of 7.4–13 km [11, 29]. The depth of the focal area, in accordance with the data on the depth of the hypocenters of the main shock and the strongest aftershocks, does not exceed 15–20 km of the upper part of the earth's crust. This feature is also characteristic of the East Anatolian (Pazarcık) earthquake with a magnitude of $M_w = 7.8$ [3].

To identify the connection of the shallow depth of the both earthquakes hypocenters with the state of the Earth's crust and the upper mantle of the region, we used the MITP08 seismotomographic model [20]. Based on this model, we have constructed a structural map for the top of the lower part of the Earth's crust and upper mantle hot volumes with negative δVp (Figs. 11a, 11b):

— $\delta Vp = -0.37\%$;

— $\delta Vp = -0.60\%$.

On the first structural map, the focal zones of both earthquakes appear in the area where the top of the lower part of the earth's crust and upper mantle "hot" volumes with negative δVp is located at depths of ≤30 km (Fig. 11a).

On the second structural map, the northeastern parts of both focal zones appear in an area where the top of the "hot" volumes is no deeper than 23 km, and the top sinks under the southwestern parts of both focal zones (Fig. 11b).

According to the resolution values of the topographic model used, the shape of the isosurface does not separate the structural layers in the lithosphere. It shows the general trend of δVp variations, the values of which reflect the average characteristics of the lower part of the Earth's crust and the upper mantle of the research area.

Elevated mantle volumes with lowered δVp are interpreted as "hot" and, accordingly, uncompacted and softened volumes. The decrease in δVp in the lower part of the earth crust is expressed by crustal waveguides [19].

We believe that the softening of the lower crust and upper mantle rocks of Eastern Anatolia made these horizons incapable of fragile seismogenic deformations and limited the seismogenerating layer of the region to the upper part of the Earth's crust. At the same time, the thermal effect of the raised low-velocity volumes on the seismogenerating layer lowered its viscosity and caused an increase in the amplitudes of strike-slip displacements in the northeastern parts of the focal zones of the Elbistan (Chardak) and East Anatolian (Pazarcık) earthquakes that occurred on February 6, 2023 compared with their southwestern parts.

CONCLUSIONS

As a result of the study, the authors came to the following conclusions.

(1) During the Elbistan earthquake, adjacent segments of the Chardak and Uluova faults became active, which were characterized by left-lateral dis-

placements. Seismogenic ruptures with a total length of 190 km appeared in the activated segments. Over the course of 148 km, sinistral displacements occurred along the resulting seismic fractures. The maximum amplitude of the left shift of 7.84 m was recorded slightly east of the epicenter.

(2) The distribution of strike-slip displacements along the activated fault segments is uneven. They form two maxima—in the zone of the Chardak fault with displacement amplitudes of 5.7–7.84 m and in the zone of the Uluova fault—3.5–5.1 m. Both maxima are confined to the areas of ophiolite distribution or to their contacts with the basement rocks. At the same time, fault zones at the contact or in the ophiolite thickness are expressed in compact strips with a width of several meters to the first tens of meters. In the crystalline rocks of the basement, faults begin to branch against the background of a decrease in the amplitudes of strike-slip displacements. Such a branching in the terminal part of the zone of seismogenic movements along the Uluova fault corresponds to the kinematic conditions of compensation for strike-slip displacements: in the right wall of the sinistral fault, the compensating ruptures were reverse faults reflecting the compression conditions; the normal faults and gaps dominating the northwest wall reflect the extension.

(3) The seismogenic Chardak and Uluova faults, formed in the regime of regional transpression, have a vertical or subvertical dip. These faults were formed at the late stages of regional collision and cut the gently sloping detachment structures that had arisen here earlier.

(4) Seismogenic strike-slip faults of the Elbistan and East Anatolian earthquakes represent the exits of their focuses to the earth's surface. In terms of the size of the focal zones and the amplitudes of seismogenic displacements, both earthquakes exceed the average values of these parameters for continental strike-slip earthquakes. At the same time, both focuses do not extend deeper than the upper part of the earth crust (16–20 km). Ophiolite assemblages are widespread in the focal zones of both earthquakes and cover the same depths. We believe that the increased sizes of focal zones and displacement amplitudes of both earthquakes are due to the presence of ophiolites, which facilitate the sliding of rocks during seismic movements. We associate the location of the seismogenic layer in the region and, accordingly, the focal zones of both earthquakes in the upper part of the earth's crust with the rise of the top of rocks with reduced P-wave velocities, capturing the upper mantle and lower part of the crust and interpreted as heated rocks with reduced strength.

SUPPLEMENTARY INFORMATION

The online version contains supplementary material available at https://doi.org/10.1134/S0016852124700250.

ACKNOWLEDGMENTS

The authors are grateful to Prof. V.I. Popkov (Kuban University, Krasnodar, Russia) and anonymous reviewer for useful comments and to editor M.N. Shoupletsova (GIN RAS, Moscow, Russia) for careful editing.

FUNDING

The heading of the article "Geological essay" was prepared as part of work on the topic FMMG-2023-0006 of the Geological Institute of the Russian Academy of Sciences. Analysis of ophiolites and heterogeneities in the structure of the earth's crust lower part and upper mantle was carried out with the support of the Russian Foundation for Basic Research, grant no. 20-55-56004/20. The rest of the research and writing of the article was carried out with funds from the Russian Science Foundation, project no. 22-17-00249.

CONFLICT OF INTEREST

The authors of this work declare that they have no conflicts of interest.

REFERENCES

1. A. C. Akinci, A. G. F. Robertson, and U. C. Ünlügenç, "Sedimentary and structural evidence for the Cenozoic subduction–collision history of the Southern Neotethys in NE Turkey (Çağlayancerit area)," Int. J. Earth Sci. (Geol. Rundsch.) **105**, 315–337 (2016).
2. M. Balkaya, H. Akyüz, and S. Özden, "Paleoseismology of the Sürgü and Çardak Faults—Splays of the Eastern Anatolian Fault Zone, Türkiye," Turkish J. Earth Sci. **32**, 402–420 (2023). https://doi.org/10.55730/1300-0985.1851
3. H. Çelik, Y. I. Trikhunkov, S. A. Sokolov, et al., "Tectonic aspects of the East Anatolian 06.02.2023 earthquake in Turkey," Izv., Phys. Solid Earth **59** (6), 822–838 (2023). https://doi.org/10.1134/S1069351323060058
4. S. Çolak, E. Aksoy, A. Koçyiğit, and M. İnceöz, "The Palu-Uluova strike-slip basin in the East Anatolian Fault System, Turkey: Its transition from the Palaeotectonic to Neotectonic stage," *Turkish J. Earth Sci.* **21**, 547–570 (2012). https://doi.org/10.3906/yer-1002-14
5. T. Danelian, G. Galoyan, Y. Rolland, and M. Sosson, "Palaeontological (radiolarian) Late Jurassic age constraint for the Stepanavan ophiolite (Lesser Caucasus, Armenia)," Bull. Geol. Soc. Greece **40** (1), 31–38 (2007). https://doi.org/10.12681/bgsg.16332
6. T. Y. Duman, Ö. Emre "The East Anatolian Fault: geometry, segmentation and jog characteristics," Spec. Publ.—Geol. Soc. London **372** (1), 495–529 (2013). https://doi.org/10.1144/SP372.14
7. O. Emre, T. Y. Duman, S. Ozalp, H. Elmasi, Ş. Olgun, and F. Şaroğlu, *Active Fault Map of Turkey with an Explanatory Text. 1 : 1250000 Scale* (General Direct. Miner. Res. Explor., Ankara, Turkey, 2013).

8. G. Galoyan, Y. Rolland, M. Sosson, M. Corsini, and R. Melkonyan, "Evidence for superposed MORB, oceanic plateau and volcanic arc series in the Lesser Caucasus (Stepanavan, Armenia)," C. R. Geosci. **339** (7), 482–492 (2007). https://doi.org/10.1016/j.crte.2007.06.002
9. *Geological Map of Turkey. 1 : 500000 Scale. Sheets: Adana, Erzurum, Hatay, Kars, Samsun, Sivas, Trabson, Van*, Ed. by M. Şenel (General Direct. Miner. Res. Explor., Ankara, Turkey, 2002).
10. *Geoscope Observatoire* (French Global Network of Broad Band Seismic Stations, Inst. Phys. Globe Paris and Ecole Observatoire Sci. Terre Strasbourg, France, 1982). (Accessed October 1, 2023). https://doi.org/10.18715/GEOSCOPE.G
11. U. Hancılar, K. Şeşetyan, E. Çaktı, et al., "Kahramanmaraş–Gaziantep Turkey $M = 7.7$ earthquake, February 6, 2023 (04:17 GMT+03:00)," in *Strong Ground Motion and Building Damage Estimations Preliminary Report (Vol. 6)* (Boğazici Univ., Kandilli Observ., Turkey, 2023).
12. E. Herece, *Atlas of the East Anatolian Fault* (General Direct. Miner. Res. Explor., Spec. Publ. Ser., Ankara, Turkey, 2008).
13. K. Hessami, H. A. Koyi, C. J. Talbot, H. Tabasi, and E. Shabanian, "Progressive unconformities within an evolving foreland fold–thrust belt, Zagros Mountains," J. Geol. Soc. **158** (6), 969–981 (2001). https://doi.org/10.1144/0016-764901-007
14. *HGM-GeoPortal* (Ministry of Nation, Defense General Direct. of Mapping, Ankara, Turkey, 2018). https://geoportal.harita.gov.tr (Accessed April 5, 2023).
15. Hole-filled SRTM for the Globe v. 4, available from the CGIAR-CSI SRTM 90m Database, (2008). https://srtm.csi.cgiar.org (Accessed March 10, 2010).
16. T. P. Ivanova and V. G. Trifonov, "New aspects of the relationship between tectonics and seismicity," Dokl. Earth Sci. **331** (5), 587–589 (1993).
17. A. L. Knipper, M. A. Satian, and N. Y. Bragin, "Upper Triassic–Lower Jurassic volcanogenic-sedimentary sediments of the Old Zod Pass (Transcaucasia)," Stratigr. Geol. Correl. **5** (3), 257–264 (1997).
18. A. Koç and N. Kaymakcı, "Kinematics of Sürgü Fault Zone (Malatya, Turkey): A remote sensing study," J. Geodynam. **65**, 292–307 (2013). https://doi.org/10.1016/j.jog.2012.08.001
19. G. V. Krasnopevtseva, *Deep Structure of the Caucasian Seismically Active Region*, Ed. by E. V. Karus (Nauka, Moscow, Russia. 1984).
20. C. Li, R. D. van der Hilst, E. R. Engdahl, and S. Burdick, "A new global model for *P*-wave speed variations in Earth's mantle," Geochem. Geophys. Geosyst. **9**, 1–21 (2008).
21. *Neotectonics, Recent Geodynamics and Seismic Hazard of Syria*, Ed. by V. G. Trifonov (GEOS, Moscow, Russia. 2012).
22. A. Robertson, O. Parlak, and T. Ustaömer, "Overview of the Palaeozoic–Neogene evolution of Neotethys in the Eastern Mediterranean region (Southern Turkey, Cyprus, Syria)," Petrol. Geosci. **18** (4), 381–404 (2012). https://doi.org/10.1144/petgeo2011-091
23. Y. Rolland, G. Galoyan, M. Sosson, R. Melkonyan, and A. Avagyan, "The Armenian ophiolite: insights for Jurassic back-arc formation, Lower Cretaceous hot spot magmatism, and Upper Cretaceous obduction over the South Armenian Block," in *Sedimentary Basin Tectonics from the Black Sea and Caucasus to the Arabian Platform*, Ed. by M. Sosson, N. Kaymakci, R.A. Stephenson, (Spec. Publ.—Geol. Soc. London, **Vol. 340**, 2010), pp. 353–382.
24. A. M. C. Sengör and Y. Yilmaz, "Tethyan evolution of Turkey: A plate tectonic approach," Tectonophysics **75**, 181–241 (1981).
25. S. Yu. Sokolov, "The depth geodynamic state and its correlation with the surface geological and geophysical parameters along the sublatitudinal profile of Eurasia," Geodynam. Tectonophys. **10** (4), 945–957 (2019). https://doi.org/10.5800/GT-2019-10-4-0451
26. M. Sosson, Y. Rolland, C. Muëller, T. Danelian, R. Melkonyan, S. Kekelia, S. Adamia, V. Babazadeh, T. Kangarli, A. Avagyan, G. Galoyan, and J. Mozar, "Subductions, obduction and collision in the Lesser Caucasus (Armenia, Azerbaijan, Georgia), new insights," in *Sedimentary Basin Tectonics from the Black Sea and Caucasus to the Arabian Platform*, Ed. by M. Sosson, N. Kaymakci, R.A. Stephenson, et al. (Spec. Publ.—Geol. Soc. London., Vol. 340, 2010), pp. 329–352.
27. V. G. Trifonov, H. Çelik, A. N. Simakova, D. M. Bachmanov, P. D. Frolov, Ya. I. Trikhunkov, A. S. Tesakov, V. M. Titov, V. A. Lebedev, D. V. Ozherelyev, A. V. Latyshev, and E. K. Sychevskaya, "Pliocene–Early Pleistocene history of the Euphrates valley applied to Late Cenozoic environment of the northern Arabian Plate and its surrounding, eastern Turkey," Quat. Int. **493**, 137–165 (2018). https://doi.org/10.1016/j.quaint.2018.06.009
28. V. G. Trifonov, S. Y. Sokolov, S. A. Sokolov, and K. Hessami, "Mesozoic–Cenozoic structure of the Black Sea–Caucasus–Caspian region and its relationships with the upper mantle structure," Geotectonics **54** (3), 331–355 (2020). https://doi.org/10.1134/S0016852120030103
29. USGS Earthquake Hazard Program, US Geol. Surv. Earthquake Hazards Program Catalog. https://earthquake.usgs.gov/earthquakes/eventpage/us6000jlqa/executive (Accessed October, 2023).
30. D. L. Wells and K. J. Coppersmith, "New empirical relationships among magnitude, rupture length, rupture width, rupture area, and surface displacement," GSA Bull. **84** (4), 974–1002 (1994). https://doi.org/10.1785/BSSA0840040974